

## OPTIMUM DESIGN OF STRUCTURES UNDER SEISMIC LOADING

**Manolis Papadrakakis, Nikos D. Lagaros, and Vagelis Plevris**

Institute of Structural Analysis & Seismic Research

National Technical University Athens

Zografou Campus, Athens 15773, Greece

e-mail: [mpapadra@central.ntua.gr](mailto:mpapadra@central.ntua.gr)

**Key words:** Structural optimization, Evolution Strategies, Seismic loading.

**Abstract.** *The objective of this paper is to perform structural optimization under seismic loading. Combinatorial optimization methods and in particular algorithms based on evolution strategies (ESs) are implemented for the solution of large-scale structural optimization problems under seismic loading. In this work the efficiency of a rigorous approach in treating dynamic loading is investigated and compared with a simplified dynamic analysis in the framework of finding the optimum design of a structure with the minimum weight. In this context a number of accelerograms are produced from the design spectrum of the region. These accelerograms constitute the multiple loading conditions under which the structures are optimally designed. This approach is compared with an approximate design approach based on simplifications adopted by the seismic codes. The results obtained for a characteristic test problem indicate a substantial improvement in the final design when the proposed optimization procedure is implemented.*

## 1 INTRODUCTION

Optimization of large-scale structures, such as sizing optimization of multi-storey 3-D frames is a computationally intensive task. The optimization problem becomes more intensive when dynamic loading is involved. In sizing optimization the aim is to minimize the weight of the structure under certain restrictions imposed by design codes. When a gradient-based optimizer is used the most time-consuming part of the optimization process is devoted to the sensitivity analysis phase which is an important ingredient of all mathematical programming optimization methods<sup>1</sup>. On the other hand the application of combinatorial optimization methods based on probabilistic searching, such as evolution strategies (ESs), do not need gradient information and therefore avoid performing the computationally expensive sensitivity analysis step<sup>2</sup>. Furthermore, it is widely recognized that combinatorial optimization techniques are in general more robust and present a better global behavior than mathematical programming methods. They may suffer, however, from a slow rate of convergence towards the global optimum.

During the last fifteen years there has been a growing interest in problem solving systems based on algorithms, which rely on analogies to natural processes. The best known algorithms in this class include evolutionary programming (EP)<sup>3</sup>, genetic algorithms (GAs)<sup>4,5</sup>, and evolution strategies (ESs)<sup>6,7</sup>. Evolution-based algorithms maintain a population of potential solutions. These algorithms have some selection process based on fitness of individuals and some recombination operators. Both ESs and GAs imitate biological evolution in nature and combine the concept of artificial survival of the fittest with evolutionary operators to form a robust search mechanism.

In the case of earthquake loading the optimization of the structural systems requires the solution of the dynamic equations of motion which can be orders of magnitude more computational intensive than the case of static loading. Moreover, due to the uncertain nature of the earthquake loading, structural designs are based on design spectra of the region of the structure and on some simplified assumptions of the structural behavior under earthquake. In this work the efficiency of a more rigorous approach with respect to the loading condition is implemented and compared with the simplified one in the framework of finding the optimum design of a structure having the minimum weight. In this context a number of accelerograms are produced from the design spectrum of the region, which constitutes the multiple loading conditions under which the structures is optimally designed. This approach is compared with the approximate one based on simplifications adopted by the seismic codes. The results obtained for a characteristic test problem indicate a substantial improvement in the final design when the rigorous approach is considered. The structural optimization problems under dynamic constraints reveal a special feature: the feasible design space is often disconnected or disjoint<sup>8,9</sup>. This feature causes difficulties for many conventional optimization methods.

## 2 FORMULATION OF THE OPTIMIZATION PROBLEM

In sizing optimization problems the aim is usually to minimize the weight of the structure under certain behavioral constraints on stress and displacements. The design variables are

most frequently chosen to be dimensions of the cross-sectional areas of the members of the structure. Due to engineering practice demands the members are divided into groups having the same design variables. This linking of elements results in a trade-off between the use of more material and the need of symmetry and uniformity of structures due to practical considerations. Furthermore, it has to be taken into account that due to fabrication limitations the design variables are not continuous but discrete since cross-sections belong to a certain set.

A discrete structural optimization problem can be formulated in the following form:

$$\begin{aligned} \min \quad & F(s) \\ \text{subject to} \quad & g_j(s) \leq 0 \quad j = 1, \dots, m \\ & s_i \in R^d, \quad i = 1, \dots, n \end{aligned} \quad (1)$$

where  $R^d$  is a given set of discrete values and the design variables  $s_i$  ( $i=1, \dots, n$ ) can take values only from this set. In the present study the sizing optimization of multi-storey 3-D frames is investigated. Optimal designs of frames have been studied initially using conventional plastic design methods. Then more sophisticated optimization algorithms were introduced in order to solve this type of problems more efficiently<sup>10,11</sup>. Most frequently the objective function is the weight of the structure and the constraints are the member stresses and nodal displacements or inter-storey drifts. For rigid frames with rolled W-shapes, the stress constraints, under allowable stress design requirements specified by Eurocode 3<sup>12</sup>, are expressed by the non-dimensional ratio  $q$  of the following formulas:

$$q = \frac{f_a}{F_a} + \frac{f_b^y}{F_b^y} + \frac{f_b^z}{F_b^z} \leq 1.0 \quad \text{if } \frac{f_a}{F_a} \leq 0.15 \quad (2)$$

and

$$q = \frac{f_a}{0.60 \cdot \sigma_y} + \frac{f_b^y}{F_b^y} + \frac{f_b^z}{F_b^z} \leq 1.0 \quad \text{if } \frac{f_a}{F_a} > 0.15 \quad (3)$$

Where  $f_a$  is the computed compressive axial stress,  $f_b^y, f_b^z$  are the computed bending stresses for y and z axis, respectively.  $F_a$  is the allowable compressive axial stress,  $F_b^y, F_b^z$  are the allowable bending stresses for y and z axis, respectively, and  $\sigma_y$  is the yield stress of the steel. The allowable inter-storey drift is limited to 1.5% of the height of each storey. One load case is considered in all examples.

### 3 STRUCTURAL DESIGN UNDER SEISMIC LOADING

The equations of equilibrium for a finite element system in motion can be written in the usual form

$$M(s_i)\ddot{u}_t + C(s_i)\dot{u}_t + K(s_i)u_t = R_t \quad (4)$$

where  $M(s_i)$ ,  $C(s_i)$ , and  $K(s_i)$  are the mass, damping and stiffness matrices for the  $i$ -th design vector  $s_i$ ;  $R_t$  is the external load vector, while  $u$ ,  $\dot{u}$  and  $\ddot{u}$  are the displacement, velocity, and acceleration vectors, respectively of the finite element assemblage. The solution methods of response spectrum modal analysis, which is based on the mode superposition approach and direct integration of the equations of motion will be considered in this work.

### 3.1 Direct time integration approach-The Newmark Method

The Newmark integration scheme is adopted in the present study to perform the direct time integration of the equations of motion. Under this scheme the variation of velocity and displacement are given by

$$\dot{u}_{t+\Delta t} = \dot{u}_t + [(1-\delta)\ddot{u}_t + \delta\ddot{u}_{t+\Delta t}]\Delta t \quad (5)$$

$$u_{t+\Delta t} = u_t + \dot{u}_t\Delta t + [(1/2 - \alpha)\ddot{u}_t + \alpha\ddot{u}_{t+\Delta t}]\Delta t^2 \quad (6)$$

where  $\alpha$  and  $\delta$  are parameters that can be determined to obtain integration accuracy and stability. When  $\delta = 1/2$  and  $\alpha = 1/6$ , relations (5) and (6) correspond to the linear acceleration method. In addition to (5) and (6), for solution of the displacements, velocities, and accelerations at time  $t + \Delta t$ , the equilibrium equations (4) at time  $t + \Delta t$  are also considered

$$M(s_i)\ddot{u}_{t+\Delta t} + C(s_i)\dot{u}_{t+\Delta t} + K(s_i)u_{t+\Delta t} = R_{t+\Delta t} \quad (7)$$

Solving from (5) for  $\ddot{u}_{t+\Delta t}$  in terms of  $u_{t+\Delta t}$  and then substituting for  $\dot{u}_{t+\Delta t}$  into (5), we obtain equations for  $\ddot{u}_{t+\Delta t}$  and  $\dot{u}_{t+\Delta t}$  each in terms of the unknown displacements  $u_{t+\Delta t}$  only. These two relations for  $\ddot{u}_{t+\Delta t}$  and  $\dot{u}_{t+\Delta t}$  are substituted into Eq. (7) to solve for  $u_{t+\Delta t}$  after using (5) and (6),  $\ddot{u}_{t+\Delta t}$  and  $\dot{u}_{t+\Delta t}$  can be also be calculated. As a result of this substitution the following well-known equilibrium equation is obtained at each  $\Delta t$ :

$$K_{\text{eff}}(s_i)u_{t+\Delta t} = R_{t+\Delta t}^{\text{eff}} \quad (8)$$

where:

$$K_{\text{eff},i} = K_i + \alpha_0 M_i + \alpha_1 C_i$$

$$R_{t+\Delta t}^{\text{eff}} = R_{t+\Delta t} + M_i(\alpha_0 \ddot{u}_t + \alpha_2 \dot{u}_t + \alpha_3 \ddot{u}_t) + C_i(\alpha_1 \dot{u}_t + \alpha_4 \ddot{u}_t + \alpha_5 \ddot{u}_t)$$

with  $\delta \geq 0.50$ ;  $\delta \geq 0.25(0.5 + \delta)^2$ ,  $\alpha_0 = \frac{1}{\alpha\Delta t^2}$ ,  $\alpha_1 = \frac{\delta}{\alpha\Delta t}$ ,  $\alpha_2 = \frac{1}{\alpha\Delta t}$ ,  $\alpha_3 = \frac{1}{2\alpha} - 1$ ,  $\alpha_4 = \frac{\delta}{\alpha} - 1$ ,

$$\alpha_5 = \frac{\Delta t}{2} \left( \frac{\delta}{\alpha} - 2 \right), \alpha_6 = \Delta t(1 - \delta), \alpha_7 = \delta\Delta t.$$

### 3.2 Creation of artificial accelerograms

The selection of the proper external loading  $R_t$  for design purposes is not an easy task due to the uncertainties involved in the seismic loading. For this reason a rigorous treatment of the seismic loading is to assume that the structure is subjected to a set of earthquakes that are more likely to occur in the region where the structure is located.

The seismic excitations that are more likely to occur are based on artificial accelerograms. In order to be representatives these artificial accelerograms that will load the structure have to match some requirements of the seismic codes. The most demanding one is that the accelerograms have to be compatible with the response spectrum of the region where the structure is located. It is well known that each accelerogram corresponds to a single response spectrum that can be defined relatively easy. On the other hand on each response spectrum corresponds an infinite number of accelerograms.

The creation of artificial accelerograms that correspond to a specific response spectrum was originally proposed by D. Gasparini and E. Vanmarke<sup>13,14</sup>. In this work the implementation published by C.A. Taylor<sup>15</sup> for the generation of statistically independent artificial acceleration time histories is adopted. This method is based on the fact that any periodic function can be expanded into a series of sinusoidal waves:

$$x(t) = \sum_k A_k \sin(\omega_k t + \varphi_k) \quad (9)$$

where  $A_k$  is the amplitude,  $\omega_k$  is the cyclic frequency and  $\varphi_k$  is the phase angle of the  $k$ -th contributing sinusoid. By fixing an array of amplitudes and then generating different arrays of phase angles, different motions can be generated which are similar in general appearance but different in the “details”. The computer uses a random number generator subroutine to produce strings of phase angles with a uniform distribution in the range between 0 and  $2\pi$ . The amplitudes  $A_k$  are related to the spectral density function in the following way:

$$G(\omega_k)\Delta\omega = \frac{A_k^2}{2} \quad (10)$$

where  $G(\omega_k)\Delta\omega$  may be interpreted as the contribution to the total power of the motion from the sinusoid with frequency  $\omega_k$ . The power of the motion produced by Eq. (9) does not vary with time. To simulate the transient character of real earthquakes, the steady-state motion are multiplied by a deterministic envelope function  $I(t)$ :

$$Z(t) = I(t)\sum_k A_k \sin(\omega_k t + \varphi_k) \quad (11)$$

The resulting motion is stationary in frequency content with peak acceleration close to the target peak acceleration. In this study a trapezoidal intensity envelope function is adopted. The generated peak acceleration is artificially modified to match the target peak acceleration, which corresponds to the chosen response spectrum. An iterative procedure is implemented to smooth the calculated spectrum and improve the matching<sup>15</sup>.

The response spectrum considered in the current study is depicted in Figure 1. Five artificial uncorellated accelerograms, produced by the previously discussed procedure and shown in Figures 2-6, have been used as the input seismic excitation for the numerical tests. The corresponding response spectrum of the first artificial accelerogram is also depicted in Figure 1.

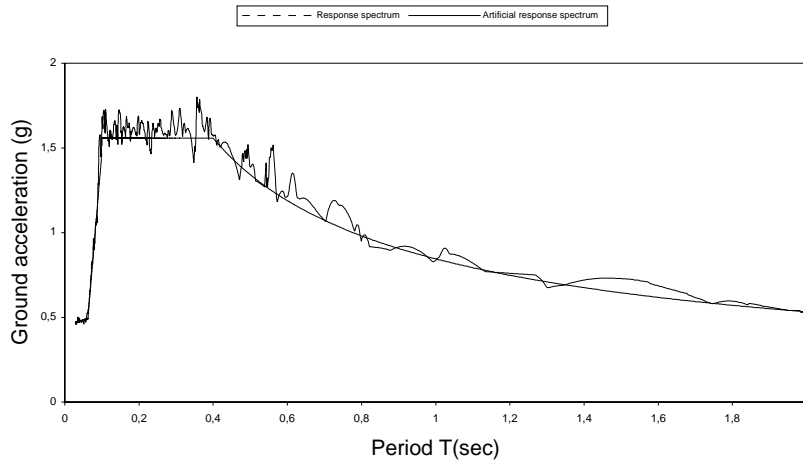


Figure 1: Response spectrum of the region and of the first artificial accelerogram

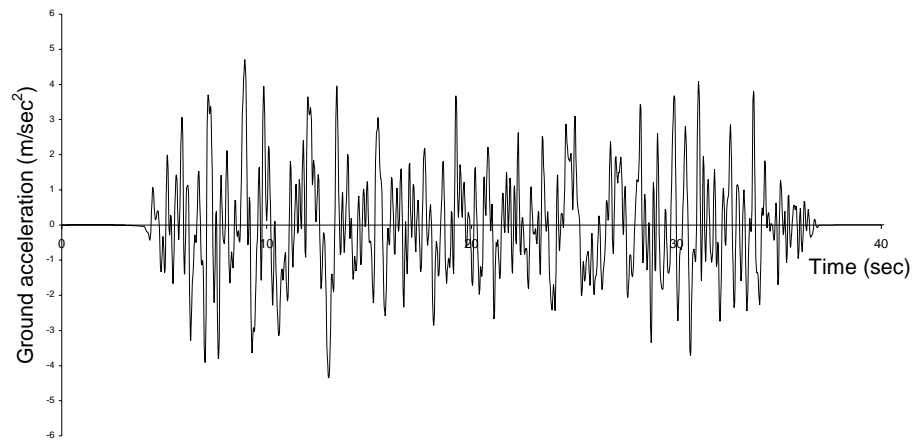


Figure 2: First artificial accelerogram

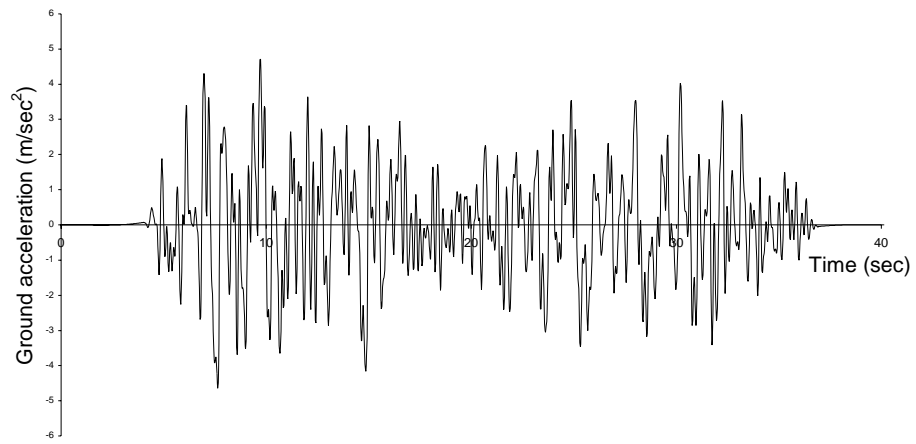


Figure 3: Second artificial accelerogram

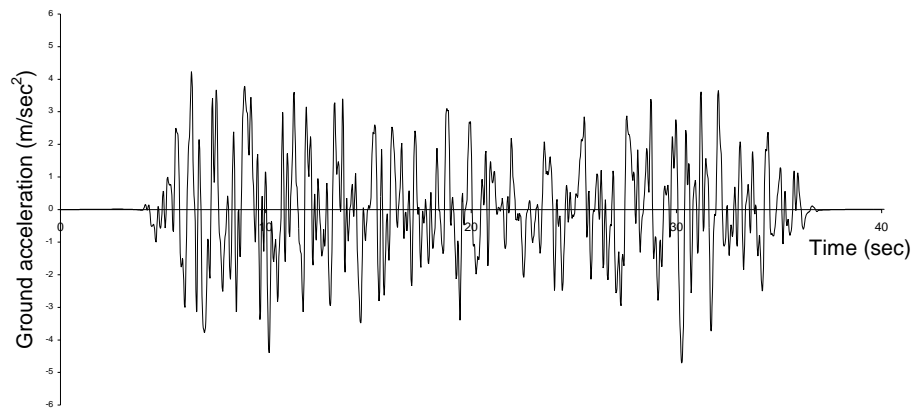


Figure 4: Third artificial accelerogram

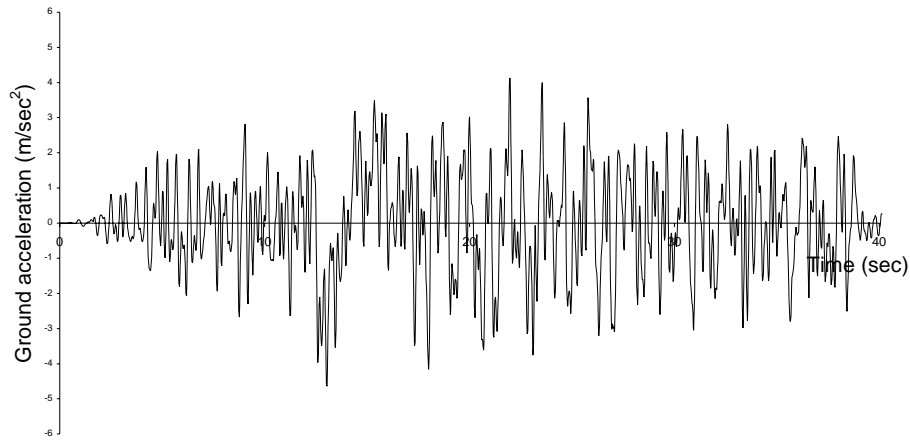


Figure 5: Fourth artificial accelerogram

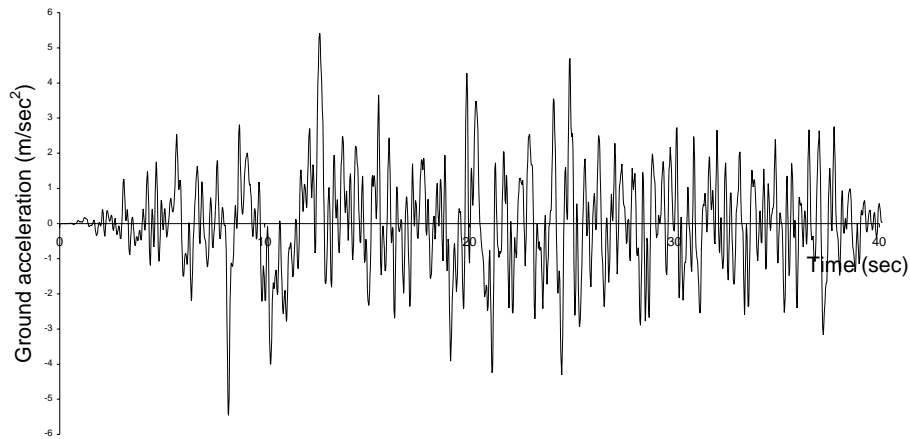


Figure 6: Fifth artificial accelerogram

### 3.3 Response spectrum modal analysis

The response spectrum modal analysis is based on a simplification of the mode superposition approach with the aim to avoid time history analyses, which are required by both the direct integration and mode superposition approaches. In the case of the response spectrum modal analysis Eq. (4) is modified according to the modal superposition approach in the following form

$$\overline{\mathbf{M}}(s_i)\ddot{\mathbf{u}}_t + \overline{\mathbf{C}}(s_i)\dot{\mathbf{u}}_t + \overline{\mathbf{K}}(s_i)\mathbf{u}_t = \overline{\mathbf{R}}_t \quad (12)$$



where

$$\bar{M}_i = \Phi_i^T M_i \Phi_i \quad (13)$$

$$\bar{C}_i = \Phi_i^T C_i \Phi_i \quad (14)$$

$$\bar{K}_i = \Phi_i^T K_i \Phi_i \quad (15)$$

$$\bar{R}_t = \Phi_i^T R_t \quad (16)$$

are the generalized values of the corresponding matrices and loading vector, while  $\Phi_i$  is an eigenmode shape matrix to be defined later. For simplicity  $M(s_i)$ ,  $C(s_i)$ ,  $K(s_i)$  are substituted by  $M_i$ ,  $C_i$ ,  $K_i$ , respectively. These matrices correspond to the design, which is defined by the  $i$ -th vector of the design parameters also called design vector.

According to the modal superposition approach the system of  $N$  simultaneous differential equations, which are coupled with the off-diagonal terms in the mass, damping and stiffness matrices, is transformed to a set of  $N$  independent normal-coordinate equations. The dynamic response can therefore be obtained by solving separately for the response of each normal (modal) coordinate and then superimposing these to obtain the response in the original coordinates.

A number of different formulas have been proposed to obtain reasonable estimates of the maximum response based on the spectral values without performing time history analyses for a large number of transformed dynamic equations. The simplest and most popular of these is the square root of the sum of the squares (SRSS) of the modal responses. According to this estimate the maximum total displacement is approximated by

$$u_{\max} = \sqrt{u_{1,\max}^2 + u_{2,\max}^2 + \dots + u_{N,\max}^2} \quad (17)$$

where  $u_{j,\max}$  corresponds to the maximum displacement calculated from the  $j$ -th transformed dynamic equations over the complete time period. The use of the Eq. (17) permits this type of “dynamic” analysis by knowing only the maximum modal coordinates  $u_{j,\max}$ .

The basic idea behind mode superposition approach and consequently the response spectrum modal analysis is to transform the set of  $N$  coupled equations of motion into a set of  $N$  uncoupled equations which can be handled more easily. The following steps summarize the response spectrum modal analysis adopted by many seismic codes around the world:

1. Calculate a number  $m' < N$  of eigenfrequencies  $\omega_i$  and the corresponding eigenmode shape matrices  $\Phi_i$ , which are classified in the following order ( $\omega_1 < \omega_2 < \dots < \omega_{m'}$ ). This is a user specified number, based on experience or on previous test analyses, which has to satisfy the requirement of step 6.
2. Calculate the generalized masses, according to the following equation

$$\bar{m}_i^j = \phi_i^{jT} M_i \phi_i^j \quad (18)$$

where  $\Phi_i = [\phi_i^1, \phi_i^2, \dots, \phi_i^{m'}]$  is the eigenmode shape matrix while  $\phi_i^j$  is the  $j$ -th eigenmode corresponding to the  $i$ -th design vector.

3. Calculate the coefficients  $L_i^j$ , according to the following equation

$$L_i^j = \phi_i^{jT} M_i r \quad (19)$$

where  $r$  is the influence vector which represents the displacements of the masses resulting from static application of a unit ground displacement.

4. Calculate the modal participation factor  $\Gamma_i^j$ , according to the following equation

$$\Gamma_i^j = \frac{L_i^j}{m_i^j} \quad (20)$$

5. Calculate the effective modal mass for each design vector and for each eigenmode, by the following equation

$$m_{\text{eff},i}^j = \frac{L_i^j{}^2}{m_i^j} \quad (21)$$

6. Calculate a number  $m < m'$  of important eigenmodes. According to the Eurocode the minimum number of the eigenmodes that has to be taken into consideration is defined by the following assumption: The sum of the effective eigenmasses must be not less than the 90% of the total vibrating mass  $m_{\text{tot}}$  of the system, so the first  $m$  eigenmodes that satisfy the equation

$$\sum_{j=1}^m m_{\text{eff},i}^j \geq 0.90 m_{\text{tot}} \quad (22)$$

are taken into consideration.

7. Calculate the values of the spectral acceleration  $R_d(T_j)$  that correspond to each eigenperiod  $T_j$  of the important modes.  
8. Calculate the modal displacements according to equation

$$(SD)_j = \frac{R_d(T_j)}{\omega_j^2} = \frac{R_d(T_j) \cdot T_j^2}{4\pi^2} \quad (23)$$

9. Calculate the modal displacements

$$u_{j,\text{max}} = \Gamma_i^j \cdot \phi_i^j \cdot (SD)_j \quad (24)$$

10. The total maximum displacement is calculated by superimposing the maximum modal displacements according to Eq. (17).

## 4 SOLUTION OF THE OPTIMIZATION PROBLEM

There are three types of algorithms belonging to the class of evolutionary computation that imitate nature by using biological methodologies in order to find the optimum solution of a problem: (i) evolutionary programming (EP), (ii) genetic algorithms (GAs) and (iii) evolution strategies (ESs). Their main difference is that GAs deal with bit-strings of fixed sizes, ES with real vectors and EP with finite state automata. GAs basic assumption is that the optimal solution can be found by assembling building blocks, i.e. partial pieces of solutions, while ESs and EP simply ensure the emergence of the best solutions. The most important consequence of this different approach is related to the recombination operator, viewed as essential for GA, as potentially useful for ES and as possibly harmful for EP. The modern tendencies seem to follow combinations of the two approaches, since GA users have turned to real number representations when dealing with real numbers following experimental results or heuristic demonstrations, whereas ES users have included recombination as a standard operator, and have designed special operators for non real-valued problems<sup>16</sup>.

Rechenberg<sup>6</sup> and Schwefel<sup>7</sup> proposed evolution strategies for parameter optimization problems in the seventies. Similar to genetic algorithms, ES imitate biological evolution in nature and have three characteristics that make them differ from other conventional optimization algorithms: (i) in place of the usual deterministic operators, they use randomized operators: mutation, selection as well as recombination; (ii) instead of a single design point, they work simultaneously with a population of design points in the space of variables; (iii) they can handle continuous, discrete and mixed optimization problems. The second characteristic allows for a natural implementation of ES on parallel computing environments. The ES, however, achieve a high rate of convergence than GA due to their self-adaptation search mechanism and are considered more efficient for solving real world problems<sup>17</sup>. The ES were initially applied for continuous optimization problems, but recently they have also been implemented in discrete and mixed optimization problems.

### 4.1 ESs for discrete optimization problems

In engineering practice the design variables are not continuous because usually the structural parts are constructed with certain variation of their dimensions. Thus design variables can only take values from a predefined discrete set. For the solution of discrete optimization problems a modified ESs algorithm has been proposed by Thierauf and Cai<sup>18</sup>. The basic differences between discrete and continuous ESs are focused on the mutation and the recombination operators. The multi membered ESs (M-ESs) that is adopted in the current study uses three operators: recombination, mutation and selection operators that can be included in the algorithm as follows:

#### Step 1 (recombination and mutation)

The population of  $\mu$  parents at  $g$ -th generation produces  $\lambda$  offsprings. The genotype of any descendant differs only slightly from that of its parents. For every offspring vector a temporary parent vector  $\tilde{s} = [\tilde{s}_1, \tilde{s}_2, \dots, \tilde{s}_n]^T$  is first built by means of recombination. For

discrete problems the following recombination cases can be used:

$$\tilde{s}_i = \begin{cases} s_{\alpha,i} \text{ or } s_{\beta,i} \text{ randomly} & \text{(A)} \\ s_{m,i} \text{ or } s_{\beta,i} \text{ randomly} & \text{(B)} \\ s_{\beta,i} & \text{(C)} \\ s_{\alpha,i} \text{ or } s_{\beta,i} \text{ randomly} & \text{(D)} \\ s_{m,i} \text{ or } s_{\beta,i} \text{ randomly} & \text{(E)} \end{cases} \quad (25)$$

$\tilde{s}_i$  is the  $i$ -th component of the temporary parent vector  $\tilde{s}$ ,  $s_{\alpha,i}$  and  $s_{\beta,i}$  are the  $i$ -th components of the vectors  $s_a$  and  $s_b$  which are two parent vectors randomly chosen from the population. In case C of Eq. (25),  $\tilde{s}_i = s_{\beta,i}$  means that the  $i$ -th component of  $\tilde{s}$  is chosen randomly from the  $i$ -th components of all  $\mu$  parent vectors. From the temporary parent  $\tilde{s}$  an offspring can be created following the mutation operator.

Let us consider the temporary parent  $s_p^{(g)}$  of the generation  $g$  that produces an offspring  $s_o^{(g)}$  through the mutation operator as follows:

$$s_o^{(g)} = s_p^{(g)} + z^{(g)} \quad (26)$$

where  $z^{(g)} = [z_1^{(g)}, z_2^{(g)}, \dots, z_n^{(g)}]^T$  is a random vector. Mutation is understood to be random, purposeless events, which occur very rarely. If one interprets them, as a set of many individual events the “natural” choice is to use a probability distribution according to which small changes occur frequently, but large ones only rarely. As a result of this assumption two requirements arise together by analogy with natural evolution: (i) the expected mean value  $\xi_i$  for a component  $z_i^{(g)}$  to be zero; (ii) the variance  $\sigma_i^2$ , the average squared standard deviation from mean value, to be small. The mutation operator in the continuous version of ESs produces a normally distributed random change vector  $z^{(g)}$ . Each component of this vector has small standard deviation value  $\sigma_i$  and zero mean value. As a result of this there is a possibility that all components of a parent vector may be changed, but usually the changes are small. In the discrete version of ESs the random vector  $z^{(g)}$  is properly generated in order to force the offspring vector to move to another set of discrete values. The fact that the difference between any two adjacent values can be relatively large is against the requirement that the variance  $\sigma_i^2$  should be small. For this reason it is suggested<sup>18</sup> that not all the components of a parent vector, but only a few of them (e.g.  $\ell$ ) should be randomly changed in every generation. This means that  $n-\ell$  components of the randomly changed vector  $z^{(g)}$  will have zero value. In other words, the terms of vector  $z^{(g)}$  are derived from

$$z_i^{(g)} = \begin{cases} (\kappa + 1)\delta s_i & \text{for } \ell \text{ randomly chosen components} \\ 0 & \text{for } n - \ell \text{ other components} \end{cases} \quad (27)$$

where  $\delta s_i$  is the difference between two adjacent values in the discrete set and  $\kappa$  is a random integer number, which follows the Poisson distribution

$$p(\kappa) = \frac{(\gamma)^\kappa}{\kappa!} e^{-\gamma} \quad (28)$$

$\gamma$  is the standard deviation as well as the mean value of the random number  $\kappa$ . For a very small  $\gamma$  (e.g. 0.001) the probability that  $\kappa$  will be zero is greater than 99%. For greater values of  $\gamma$  (e.g. 0.05) the probability that  $\kappa$  will be zero is 95% and the probability that it will be one is 5%. This shows how the random change  $z_i^{(g)}$  is controlled by the parameter  $\gamma$ . The choice of  $\ell$  depends on the size of the problem and it is usually taken as the 1/5 of the total number of design variables. The  $\ell$  components are selected using uniform random distribution in every generation according to Eq. (27).

### Step 2 (selection)

There are two different types of the multi-membered ES:

( $\mu+\lambda$ )-ESs: The best  $\mu$  individuals are selected from a temporary population of ( $\mu+\lambda$ ) individuals to form the parents of the next generation.

( $\mu,\lambda$ )-ESs: The  $\mu$  individuals produce  $\lambda$  offsprings ( $\mu \leq \lambda$ ) and the selection process defines a new population of  $\mu$  individuals from the set of  $\lambda$  offsprings only.

In the second type, the life of each individual is limited to one generation. This allows the ( $\mu,\lambda$ )-ESs selection to perform better on dynamic problems where the optimum is not fixed, or on problems where the objective function is noisy.

For discrete optimization the procedure terminates when one of the following termination criteria is satisfied: (i) when the best value of the objective function in the last  $4n\mu/\lambda$  generations remains unchanged, (ii) when the mean value of the objective values from all parent vectors in the last  $2n\mu/\lambda$  generations has not been improved by less than a given value  $\varepsilon_b$  ( $=0.0001$ ), (iii) when the relative difference between the best objective function value and the mean value of the objective function values from all parent vectors in the current generation is less than a given value  $\varepsilon_c$  ( $=0.0001$ ), (iv) when the ratio  $\mu_b/\mu$  has reached a given value  $\varepsilon_d$  ( $=0.5$  to  $0.8$ ) where  $\mu_b$  is the number of the parent vectors in the current generation with the best objective function value.

## 4.2 ESs in structural optimization problems

So far comparatively little effort has been spent in applying probabilistic search methods to structural optimization problems<sup>1,19</sup>. Usually this type of problems are solved with a mathematical programming algorithm such as the sequential quadratic programming method (SQP)<sup>20,21</sup>, the generalized reduced gradient method (GrG)<sup>22</sup>, the method of moving asymptotes (MMA)<sup>23</sup>, which need gradient information. In structural optimization problems, where the objective function and the constraints are particularly highly non-linear functions of the design variables, the computational effort spent in gradient calculations is usually large.

Little effort has been also spent in examining structural optimization problems for dynamic loading and especially under earthquake loading within a certain seismic code<sup>24</sup>.

In a recent work by Papadrakakis et. al.<sup>1</sup> it was found that combinatorial type algorithms are computationally efficient even if larger number of analyses are needed to reach the optimum. These analyses are computationally less expensive than in the case of mathematical programming algorithms since they do not need gradient information. Furthermore, probabilistic methodologies, due to their random search, are considered to have a better behaviour in optimization problems with local optima since they are more capable of finding the global optimum, whereas mathematical programming algorithms may be trapped in local optima. Finally, the natural parallelism inherent in combinatorial algorithms makes them very attractive for application in parallel computer architectures.

The ESs optimization procedure starts with a set of parent vectors. If any of these parent vectors gives an infeasible design then this parent vector is modified until it becomes feasible. Subsequently, the offsprings are generated and checked if they are in the feasible region. According to  $(\mu+\lambda)$  selection scheme in every generation the values of the objective function of the parent and the offspring vectors are compared and the worst vectors are rejected, while the remaining ones are considered to be the parent vectors of the new generation. On the other hand, according to  $(\mu,\lambda)$  selection scheme only the offspring vectors of each generation are used to produce the new generation. This procedure is repeated until the chosen termination criterion is satisfied.

The number of parents and offsprings involved affects the computational efficiency of the multi-membered ESs discussed in this work. It has been observed that values of  $\mu$  and  $\lambda$  equal to the number of the design variables produce better results<sup>1</sup>. The ESs algorithm for structural optimization applications under seismic loading can be stated as follows:

1. *Selection step* :  
selection of  $s_i$  ( $i = 1, 2, \dots, \mu$ ) parent vectors of the design variables
2. *Analysis step* :  
solve  $M(s_i)\ddot{u} + C(s_i)\dot{u} + K(s_i)u = R(t)$  ( $i=1, 2, \dots, \mu$ )
3. *Constraints check* :  
all parent vectors become feasible
4. *Offspring generation* :  
generate  $s_j$ , ( $j=1, 2, \dots, \lambda$ ) offspring vectors of the design variables
5. *Analysis step* :  
solve  $M(s_j)\ddot{u} + C(s_j)\dot{u} + K(s_j)u = R(t)$  ( $j=1, 2, \dots, \lambda$ )
6. *Constraints check* :  
if satisfied continue, else change  $s_j$  and go to *step 4*
7. *Selection step* :  
selection of the next generation parents according to  $(\mu+\lambda)$  or  $(\mu,\lambda)$  selection schemes
8. *Convergence check* :  
If satisfied stop, else go to *step 3*

## 5 NUMERICAL RESULTS

One benchmark test example of space frame with six storeys has been considered to illustrate the efficiency of the proposed methodology in sizing optimization problems with discrete design variables. The modulus of elasticity is 200 GPa and the yield stress is  $\sigma_y=250$  MPa. The cross section of each member is assumed to be a W-shape and for each member two design variables are considered as shown in Figure 7. The objective function of the problems is the weight of the structure. The constraints are imposed on the inter-storey drifts and on the maximum non-dimensional ratio  $q$  of Eqs. (2) and (3) for each element group which combines axial force and bending moments. The values of allowable axial and bending stresses are  $F_a=150$  MPa and  $F_b=165$  MPa, respectively, whereas the maximum allowable inter-storey drift is limited to 4.5 cm which corresponds to 1.5% of the height of each storey. The test example was run on a Silicon Graphics Power Challenge computer.

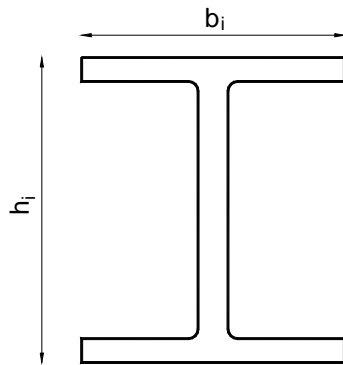


Figure 7: W-shape cross section

The space frame consists of 63 elements with 180 degrees of freedom as shown in Figure 8. The beams have length  $L_1=7.32$  m and the columns  $L_2=3.66$  m. The structure is loaded with a 19.16 kPa gravity load on all floor levels and a static lateral load of 109 kN applied at each node in the front elevation along the  $z$  direction. The element members are divided into 5 groups, as shown in Figure 8, each one having two design variables resulting in ten total design variables. The constraints are imposed on the maximum allowable inter-storey drift and the non-dimensional ratio  $q$  for each element group. For this test case both  $(\mu+\lambda)$ -ES and  $(\mu,\lambda)$ -ES schemes are implemented.

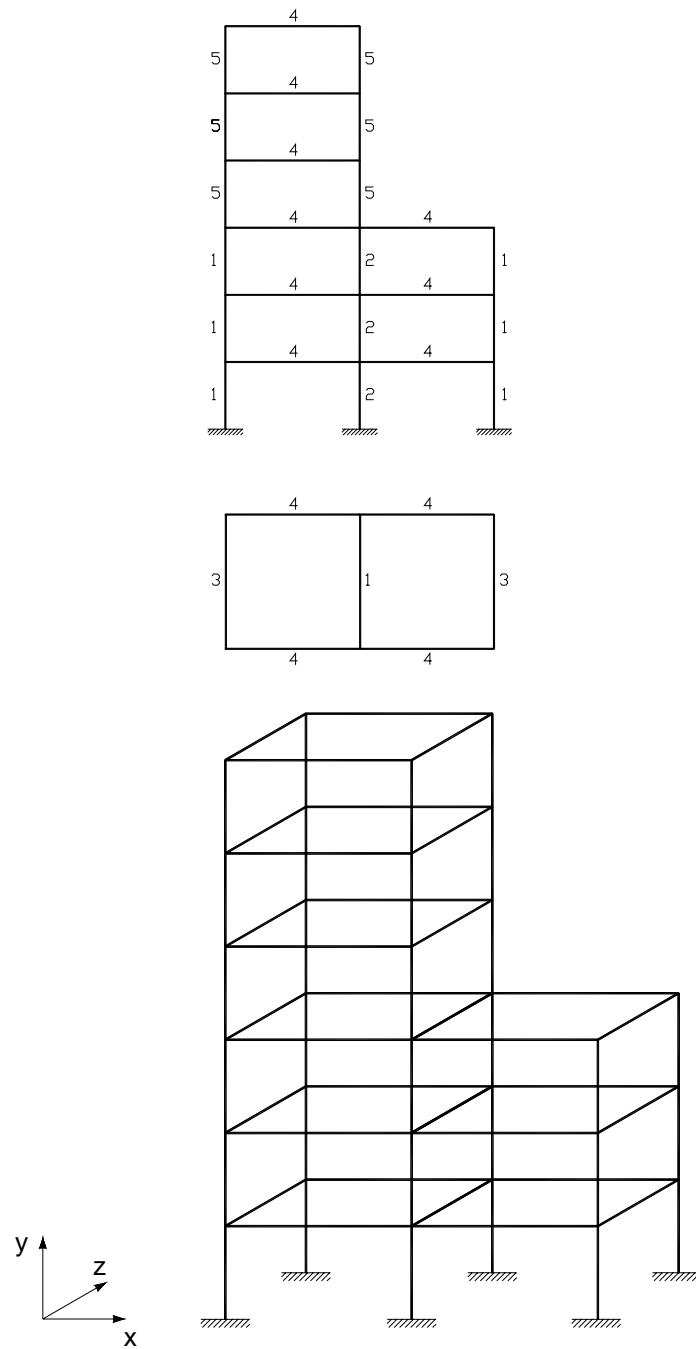


Figure 8: Six storey space frame

### 5.1 Convergence histories

The convergence history with respect to the finite element analyses performed by the



optimization procedure using the (5+5)-ESs scheme is shown in Figure 9 for the direct time integration and the response spectrum modal analysis methods.

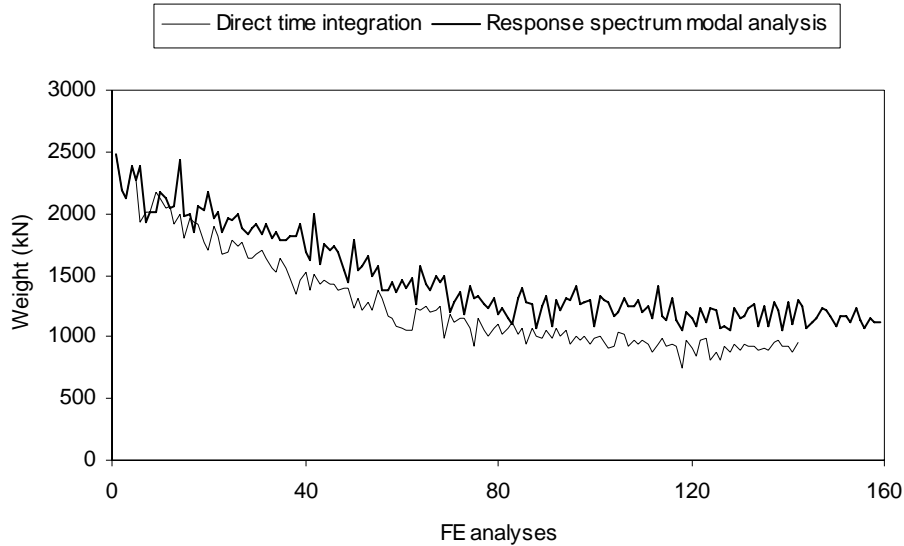


Figure 9: Convergence histories of the optimization procedure

## 5.2 Examination of the schemes $(\mu+\lambda)$ ES and $(\mu, \lambda)$ ES

In this paragraph the behaviour of  $(\mu+\lambda)$ -ESs and  $(\mu, \lambda)$ -ESs schemes with  $\mu=\lambda=5$  are compared. The upper values of the design parameters are taken as the initial design, while the termination criterion (i) is adopted for both schemes ( $W_{\text{initial}}=2486$  kN). The results obtained are shown in Table 1 for the direct integration approach and the response spectrum modal analysis. The results indicate that the  $(\mu+\lambda)$ -ESs scheme appears to be more robust than the  $(\mu, \lambda)$ -ESs scheme.

ESs scheme	Weight (kN)	Time (sec)	Generations	FE analyses						
$(\mu+\lambda)$	944	13818	40	142						
$(\mu, \lambda)$	842	39657	40	359						
Optimum solution achieved (design variables-cm)										
ESs scheme	$h_1$	$b_1$	$h_2$	$b_2$	$h_3$	$b_3$	$h_4$	$b_4$	$h_5$	$b_5$
$(\mu+\lambda)$	46	38	58	46	51	35	20	15	46	33
$(\mu, \lambda)$	51	35	46	43	51	35	30	13	51	20

(a) The  $(\mu+\lambda)$ -ESs and  $(\mu, \lambda)$ -ESs schemes for the direct time integration approach

ESs scheme	Weight (kN)	Time (sec)	Generations	FE analyses						
$(\mu+\lambda)$	1126	5674	40	157						
$(\mu, \lambda)$	1316	5284	21	140						
Optimum solution achieved (design variables-cm)										
ESs scheme	$h_1$	$b_1$	$h_2$	$b_2$	$h_3$	$b_3$	$h_4$	$b_4$	$h_5$	$b_5$
$(\mu+\lambda)$	51	41	53	53	51	41	28	20	35	33
$(\mu, \lambda)$	43	43	66	56	51	46	33	23	41	35

(b) The  $(\mu+\lambda)$ -ESs and  $(\mu,\lambda)$ -ESs schemes for the response spectrum modal analysis

Table 1 : Comparison of  $(\mu+\lambda)$ -ESs and  $(\mu,\lambda)$ -ESs schemes

### 5.3 Examination of the influence of the number of parents and offsprings

The influence of the number of parents and offsprings are considered in this paragraph. The results presented in Table 2 indicate that the schemes close to (5+5)-ESs scheme have better convergence. This confirms the empirical rule that the sum of the parents and offsprings should be roughly equal to the number of the design parameters of the problem. Schemes with larger number of parents and offsprings can give good results in some cases, as far as the optimum is concerned, but they consume much more time until they reach convergence.

ESs scheme	Weight (kN)	Time (sec)	Generations	FE analyses
(3+3)	863	9839	65	135
(3+5)	917	11308	35	113
(5+3)	963	12816	56	123
(5+5)	944	13818	40	142
(5+10)	835	20574	38	248
(10+5)	824	29363	78	306
(10+10)	844	32130	48	381

(a) Direct time integration approach

ESs scheme	Weight (kN)	Time (sec)	Generations	FE Dynamic analyses
(3+3)	1207	3110	37	82
(3+5)	1103	3527	29	92
(5+3)	1082	9853	129	299
(5+5)	1126	5674	40	157
(5+10)	1165	4897	18	130
(10+5)	1253	4154	23	109
(10+10)	1108	8646	29	235

(b) Response spectrum modal analysis

Table 2 : Influence of the number of parent and offspring for the  $(\mu+\lambda)$ -ESs schemes

#### 5.4 Examination of the influence of the initial point

The behaviour of the (5+5)-ESs scheme for different initial designs is depicted in Table 3 and 6. The initial designs correspond to one feasible and one infeasible design. The results show that the final optimum design could be affected by the initial parameters in the range of 10% at the most.

Initial design	Weight (kN)	Time (sec)	Generations	FE analyses
feasible	944	13818	40	142
infeasible	1037	9473	35	178

(a) Direct time integration approach

Initial design	Weight (kN)	Time (sec)	Generations	FE analyses
feasible	1126	5674	40	157
infeasible	1104	9510	46	246

(b) Response spectrum modal analysis

Table 3 : Influence of the starting point of the (5+5)-ESs scheme

## 6 CONCLUSIONS

The presented results indicate the substantial improvement that can be achieved in the final design of structures under seismic loading when the proposed optimization procedure is implemented. The more rigorous dynamic approach based on time history analyses for a number of artificially generated earthquakes gives more economic designs than the approximate response spectrum analysis adopted by the seismic codes, at the expense of requiring more computational effort.

## REFERENCES

- [1] Papadrakakis M., Tsompanakis Y., Hinton E., and Sienz J., "Advanced Solution Methods in Topology Optimization and Shape Sensitivity Analysis", *Journal of Engineering Computations*, **13(5)**, 57-90 (1996).
- [2] Papadrakakis M., Tsompanakis Y., and Lagaros N.D., "Structural shape optimization using Evolution Strategies", *Engineering Optimization*, **31**, 515-540 (1999).
- [3] Fogel L.J., Owens A.J., and Walsh M.J., *Artificial intelligence through simulated evolution*, Wiley, New York, 1966.
- [4] Goldberg D.E., *Genetic algorithms in search, optimization and machine learning*, Addison-Wesley Publishing Co., Inc., Reading, Massachusetts, 1989.
- [5] Holland J., *Adaptation in natural and artificial systems*, University of Michigan Press, Ann Arbor, 1975.
- [6] Rechenberg I., *Evolution strategy: optimization of technical systems according to the principles of biological evolution*, Frommann-Holzboog, Stuttgart, 1973.
- [7] Schwefel H.P., *Numerical optimization for computer models*, Wiley & Sons, Chichester, UK, 1981.
- [8] Cassis, J.H., *Optimum design of structures subjected to dynamic loads*, Ph.D. Thesis, University of California, Los Angeles, 1974
- [9] Johnson, E.H., "Disjoint design spaces in optimization of harmonically excited structures", *AIAA Journal*, **14(2)**, 259-261 (1976).
- [10] Thevendran V., Das Gupta N.C., and Tan G.H., "Minimum weight design of multi-bay multi-storey steel frames", *Comp. & Struc.*, **43(3)**, 495-503 (1992).
- [11] Barsan G.M., "Optimal design of planar frames based on structural performance criteria", *Comp. & Struct.*, **3(2)**, 1395-1400 (1994).
- [12] Eurocode 3, Design of steel structures, Part1.1: General rules for buildings, CEN, ENV 1993-1-1/1992.
- [13] Gasparini, D. A. and Vanmarke, E. H., *Simulated earthquake motions compatible with prescribed response spectra*, Massachusetts Institute of Technology (MIT), Department of Civil Engineering, Publication No. R76-4, January 1976.
- [14] Gasparini, D. A., *SIMQKE - A program for artificial motion generation, User's manual and documentation*, Massachusetts Institute of Technology (MIT), Department of Civil Engineering, November 1976.
- [15] Taylor, C. A., *EQSIM, A program for generating spectrum compatible earthquake*

- ground acceleration time histories, Reference Manual*, Bristol Earthquake Engineering Data Acquisition and Processing System, December 1989.
- [16] Schoenauer M., "Shape representation for evolutionary optimization and identification in structural mechanics", in Winter G., Periaux J., Galan M. and Cuesta P. (eds), *Genetic Algorithms in engineering and computer science*, J. Wiley, 443-464 (1995).
- [17] Hoffmeister F., and Back T., "Genetic Algorithms and Evolution Strategies-Similarities and Differences", in Schwefel, H.P. and Manner, R. (eds.), *Parallel Problems Solving from Nature*, Springer-Verlag, Berlin, Germany, 455-469 (1991).
- [18] Thierauf G., and Cai J., "Structural optimization based on Evolution Strategy", in Papadrakakis M. and Bueda G. (eds), *Advanced computational methods in structural mechanics*, CIMNE, Barcelona, 266-280 (1996).
- [19] Papadrakakis, M. and Lagaros N.D., Thierauf, G. and Cai, J.; "Advanced Solution Methods in Structural Optimization Based on Evolution Strategies", *Engineering Computations Journal*, **15**, 12-34 (1998).
- [20] Belegundu A.D., and Arora J.S., "A study of mathematical programming methods for structural optimization, Part I: Theory, Part II: Numerical results", *Int. J. Num. Meth. Engng.*, **21**, 1583-1623 (1985).
- [21] Thanedar P.B., Arora J.S., Tseng C.H., Lim O.K., and Park G.J., "Performance of some SQP methods on structural optimization problems", *Int. J. Num. Meth. Engng.*, **23**, 2187-2203 (1986).
- [22] Lasdon L.S., Warren A.D., Jain A., and Ratner R., "Design and testing of a generalized reduced gradient code for nonlinear programming", *ACM Trans. Math. Softw.*, **4(1)**, 34-50 (1978).
- [23] Svanberg K. "The method of moving asymptotes, a new method for structural optimization", *Int. J. Num. Meth. Engng.*, **23**, 359-373 (1987).
- [24] Cai J. *Discrete Optimization of Structures under Dynamic Loading by Using Sequential and Parallel Evolution Strategies*, Doctoral Dissertation, Department of Civil Engineering, University of Essen, Germany, 1995.